INSIGHT INTO DEVELOPMENT OF FINITE ELEMENT MULTI-NONLINEAR EARTH RETAINING STRUCTURE MODEL

Mohamed Elkhairy Salama

Faculty of Engineering, Garyan
Gabal Al-Garby University, Libya

الملخص

توزيع ضغط التربة خلف الحوائط الساندة تم دراسته ومنذ زمن طويل لكن العلاقة بين مقدار الضغط وقيمة الحركة الأفقية للحوائط لم يتم توثيقها نظرياً إلى حد الآن. هذه الدراسة محاولة للتعمق في تمثيل المنشآت الساندة عددياً. النموذج الذي تم تقديمه يحتوى على حائط خرساني كابولي مرن يسند تربة تم تمثيلها بنموذج دراكر–براجر. التماس بين التربة والحائط تم تمثيله بإستخدام عنصر تماس غير خطى. كما تم تمثيل جزء التربة الذي تم حفره أمام الحائط بواسطة موت عناصر التربة لهذا الجزء. تمت دراسة عدد 15 حالة وتوضيح العوامل التي تؤثر على سلوك النموذج ككل وهى زاوية الإحتكاك الداخلي للتربة وتغير معامل المرونة للتربة والحائط، ومقاومة الإحتكاك خلف الحائط. كما تم تمثيل التحكم في حركة الحائط عند الطرف السفلي للحائط وعند الطرف العلوي له. التشكل الهندسي غير الخطى للعناصر تم أخذه في الإعتبار في بعض الحالات لدراسة تأثيرها على النتائج وعلى تقارب الوصول للحل النهائي. تم مقارنة الضغط الأفقي على الحائط الناتج من الدراسة للحالات المختلفة مع نتائج توزيع رانكين و كولومب. لبيان تأثير العوامل السابقة على النتائج تم تقديم الإجهاد الرأسي في واجهة الحائط الملامسة للتربة بالإضافة إلى عزوم الإنحناء مقسومة على مرونة الإنحناء للحائط. من نتائج هذه الدراسة تم التوصل الى مقترح عام لتوزيع الضغط خلف الحوائط الخرسانية المسلحة الكابوليه.

ABSTRACT

Earth pressure distribution behind walls has been studied for a long time, but the coupling between deformation and stress is not well documented theoretically. In this study an attempt is made to introduce an insight into the modeling of earth retaining structures. The studied model is an elastic cantilever diaphragm wall, supporting nonlinear Drucker-Prager soil, and a nonlinear contact simulation between wall and soil. The excavated part of the model is simulated by element death. A total of 15 runs are presented to show different factors that influence the behavior of the retaining system (friction angle, variation of soil and wall modulus, and contact friction), and simulations of boundary conditions (lower end restraints of the wall, propped wall at the top end). Geometric nonlinearity is activated in some runs to study its influence on the result and convergence. A comparison is made between the resulted horizontal stress and that computed by Rankine and Coulomb theories. To show the influences of all different

factors, vertical stress in the inner wall face and normalized wall bending are presented. A generalized pressure distribution diagram for cantilever diaphragm wall is proposed.

KEYWORDS: Diaphragm wall; Earth pressure distribution; Nonlinear soil; Contact simulation; Geometric nonlinearity; Plastic strain; Wall stiffness bending and deflection.

INTRODUCTION

The rigorous analysis of earth pressure problems is rarely possible. The earth pressure problem considered as a problem in plasticity, which interested in failure of soil without consideration to displacement. Thus all earth pressure theories do not give the lateral movement of the wall, which support certain soil. The earth pressure theories considered an idealized soil model without specifying the required lateral movement of the walls. In literatures there are a number of semi-empirical earth pressure distribution behind retaining structures (for example; Terzaghi and Peck [1], Peck [2], and Mana and Clough [3]), some of them based on field measurements.

The problem of wall retaining soil is a complex interaction of construction method, excavation depth, and stiffness of wall, type and state of retained soil, passive resistance, restraint condition at the top of the wall, embedment length, and soil wall friction. Figure (1) shows soil-wall-load-structure nonlinear interaction presented by the author for general retaining diaphragm wall. Finite element is less of an approximation than some proposed methods of design based on assumptions of certain earth pressure distributions. Additionally it allows for better modeling of each variable mentioned above. Therefore the present study is initiated to get some insight into modeling of retaining walls non-gravity type. The study includes influence of modeling factors such as end restraints of the wall, geometric nonlinearity, contact stiffness, and developing of gap between soil and wall during the process of the solution. The influence of soil properties and wall stiffness are included also. The nonlinear solutions compared by, cumulative number of iterations, maximum lateral wall movement, number of load sub steps during the solution, and the total CPU time for the solution. Horizontal stress distribution behind the wall is presented and compared with active and at rest pressure distribution. Normalized bending moment diagrams for the wall presented to show influence of different factors on wall behavior. Based on the results of this study a pressure distribution diagram is proposed by the author. ANSYS 5.4 [4] finite element program is used in this study. Table (1) shows all the variables included in the study. It is implemented by optimizing the number of runs required to achieve all the comparative variables. The total number of runs is 15.

EARTH PRESSURE THEORIES – APPLICATION TO CANTELIVER WALLS

Plastic collapse occurs after the state of plastic equilibrium has been reached in part of soil mass, resulting in slipping of that soil mass relative to the rest of the mass. This happened in run No 1 and 3 when geometric nonlinearity was included. After 90% of the solution completed, element shape at the top edge in the plastic zone highly deformed which stops the solution by the program. The limit theorems of plasticity used to calculate lower and upper bounds to the true collapse load. In lower bound approach the condition of equilibrium and yield are satisfied, the Mohr-Coulomb failure criterion is taken to be the yield criterion. In upper bound approach choosing a slip surface forms a mechanism of plastic collapse and work done by the external force is equated to the

internal dissipation of energy. Rankin's theory of earth pressure satisfies the lower bound condition, the theory results either in an overestimation of active pressure and an underestimation of passive pressure or in exact value of active and passive pressure. The Coulomb theory is interpreted as an upper bound condition. Thus, the theory underestimates the total active thrust and overestimates the total passive resistance, Craig [5].

Earth Pressure Development and Compatibility of Deformations

BS 8002 [6] standard stated that: the maximum earth pressures on a retaining structure occurring during working conditions and the necessary equilibrium calculations are based on the assumption that earth pressures greater than fully active pressure and less than fully passive will act on the retaining structure during service. As ultimate limit state with respect to soil pressures is approached, with sufficient deformation of the structure, the active earth pressure in the retained soil reduces to the fully active pressure and the passive resistance tends to increase to the full available passive resistance.

NONLINEAR FINITE ELEMENT MODELING OF CANTELIVER DIAPHRAGM WALL

Soil behavior in literature simulated using many models for example; Modified Cam Clay model (e.g., Potts and Martins [7]) and empirical stress-strain relations (e.g., hyperbolic, Ottaviani and Marchetti, [8], logarithmic, Jardine, et. al. [9]). More sophisticated constitutive models (e.g., Ananadarajah, and Dafalias [10], Banerjee, et. al. [11], Mroz and Zienkiewicz [12], Prevost, J. H. [13]). A cantilever reinforced concrete diaphragm wall with 50 cm thickness, unsupported height 9.45 m, and embedded length in soil is10 m. The finite element mesh used in the analysis is shown in Figure (2). The model simulated using 275 PLANE82 (8-node isoparametric element for soil), 530 CONTAC48 (wall-soil contact), and 210 PLANE42 (4-node isoparametric element for wall) with modulus of elasticity varies as shown in Table (1) to study the influence of wall stiffness on wall deflections and stress distributions. The condition of plane strain is assumed as in all theories of earth pressure. It is tried to introduce treatment of simulation of earth pressure problem by considering both stresses and displacements that involved simulation of soil by nonlinear Drucker- Prager [14] soil model with associated flow rule, with nonlinear contact element between soil and wall, geometric nonlinearity is included to account for large soil displacements, and the wall is considered as elastic concrete material. In runs 3, 7 and 12 the soil modulus changed with depth. The automatic time stepping feature in ANSYS program will respond to plasticity by reducing the load step size after a load step in which a large number of equilibrium iterations was performed or in which a plastic strain increment greater than 5% was encountered. Table (1) shows the characteristics of each run and the results to be compared.

Table 1: Soil Properties, Boundary Conditions, and wall Stiffness Data for Runs 1 to 15

Run No.	Soil			Variables to be compared		Wall	Condition at tip Boundary of the wall[1]	Geometric Nonlinearity	Existence of gap	Cumulative No. of iterations	Max. lateral wall movement at top end	Contact stiffness		No of sub steps	Total CPU time[2] min
	γ kN/m^3	ϕ^o	E kN/m^2			E kN/m^2 / EI kN.m^2					U_x cm.	KN kN/m	KT kN/m		
1[3]	17.5	31	11500	Geometric nonlinearity	Runs 1,5 Change in friction angle	23x10^6 / 23x10^4	1	On	Small at bottom	278[4]	0.215266	11500	3870	117	19, 90% of solution
2	17.5	31	11500			23x10^6 / 23x10^4	1	Off	Small at bottom	170	0.23526	11500	3870	62	11
3	17.5	31	9000, 11500,13000	E, soil varied with depth	Compare with run 7	23x10^6 / 23x10^4	1	On	v. Small at bottom	328[4]	0.215289	11500	3870	194	26 93 % of solution
4	18.5	35	18000	Runs 4, 9 Change in friction angle	Wall boundary condition at wall tip	23x10^6 / 23x10^4	2	On	No Gap	105	0.126302	18000	6910	60	8
5	18.5	35	18000	Wall stiffness		23x10^6 / 23x10^4	1	On	v. Small at bottom	140	0.123855	18000	6910	62	13
6	18.5	35	18000			15x10^6 / 15x10^4	1	On	Small at bottom	175	0.136761	18000	6910	62	13
7	18.5	35	11000,18000, 35000	E, soil varied with depth	Compare with run 3 and 4	23x10^6 / 23x10^4	1	On	v. Small at bottom	254	0.107251	18000	6910	182	21
8	20	39	35000		Geometric nonlinearity	23x10^6 / 23x10^4	2	Off	Small at Top	81	0.05053	35000	15146	60	12
9	20	39	35000	Contact		23x10^6	2	On	Small at Top	88	0.050979	35000	15146	60	12

				stiffness		$23x10^4$									
10	20	39	35000			$23x10^6$ $23x10^4$	2	On	Small at Top	65	0.049705	35000	500	60	5
11	17.5	31	11500	Propped wall at top	Compare with runs 1 and 2	$23x10^6$ $23x10^4$	1	On	At top 3 element+ very small at bottom	104	0.045374(5)	11500	3870	32	7
12	18.5	35	11000,18000, 35000	Propped wall at top	Compare with run 7	$23x10^6$ $23x10^4$	1	On	At top 2 1/2 element+ very small at bottom	72	0.02637(5)	18000	6910	35	7
13	Same as Run 11 but elastic soil				Compare with run 11	$23x10^6$ $23x10^4$			At top 3 element+ very small at bottom	116	0.0402	11500	3870	81	9
14	Same as run 5 but reduced wall stiffness			Wall stiffness	Compare with run 5	$23x10^5$ $23x10^3$	1	On		240(4)	0.25727	18000	6910	88	20 84% of solution
15	Same as run 14 but with geometric nonlinearity off				Compare with run 5 and 14	$23x10^5$ $23x10^3$		Off	Very small at bottom	345	0.232002	18000	6910	155	24

(1) – 1 – free in X direction, restraints in Y direction. --2—restraints in X and Y directions
(2) Computer used with Intel Processor 500 MHz, 192 MB RAM. ----- all the analysis run with automatic time stepping
(3) After excavation (killed elements on excavation side)
(4) Non-converged solution, % of solution completed 90%, 93%, and 84%.
(5) Max. lateral movement occurs at lower level of excavation not at top end of the wall.

Contact Simulation

Several interface elements have been proposed and used in literature (e.g., Goodman et al. [15]; Zeinkiewicz et al. [16]; Ghaboussi et al. [17]; Katona [18]; Herrmann [19]; and Desai et al. [20]). Zeinkiewicz et al. [16] and Desai et al. [20] used thin conventional isoparametric elements to model interfaces. Ghaboussi et al. [17] and Wilson [21] pointed out that numerical ill-conditioning of the stiffness matrix may develop when such elements are used and suggested the use of relative displacements between adjacent nodes as independent degrees of freedom. However, Pande and Sharma [22] used both conventional and relative displacement formulation and found that if the computation is performed using high precision; both formulations yield similar results for aspect ratios of the interface elements greater than a thousand. Simulations of contact problems are highly nonlinear. Contact models available in ANSYS are: point-to-point, point-to-surface, and surface-to-surface. Before using any model to simulate a contact between the soil and the wall, one must understand the capabilities and limitations of each model. At the beginning the author used the point-to-point contact, but the results show very large deflection of the wall with large separation between the soil and the wall. It is found that this element is best suited to problems with small negligible sliding and deflections of the contact surface, and the nodes of the two surfaces match up geometrically (node-to-node contact).

Node-to-surface elements can be used to model surface-to-surface contact, if the contacting surface is defined by a group of nodes and multiple elements are generated. The exact location of the contacting area needs not to be known beforehand, nor do the contacting components need to have a compatible mesh. Large deformation and large relative sliding are allowed, although this capability can also model small sliding. The element used in this analysis is 2-D CONTAC48. Nonlinearities in this element are: surface-to-surface contact with large deformation, contact and separation, and Coulomb friction sliding. Contact elements are triangles, where the base is made up of nodes on the target surface (wall) and the remaining is a node on the contact surface (soil). The program uses contact elements to track the relative positions of the two surfaces. Midside nodes can be used on the contact surface only (soil), but not on the target surface (wall). The friction model chosen for simulation of contact between soil and wall is elastic Coulomb, which allows both sticking and sliding. Compatibility on the contact surface is accomplished by the penalty with Lagrange multiplier method; a force is applied to the contacting node until it penetrates the surface by less than an amount defined by the real constant TOLN. Maximum penetration tolerance TOLN=1%. Input real constant values are: Normal contact stiffness KN (kN/m) should be large to restraint the model from over-penetration, but not so large it cause ill-conditioning. Sticking contact stiffness should be less than the normal stiffness. The value suggested by the author is KT = tan ((1/2 to 2/3) ϕ) kN. Small tolerance that used internally by the program to increase the length of the target surface TOLS=0.5% of contact length.

RESULTS AND DISCUSSIONS

Figures (3 and 4) show example for the deformed shape for runs 11 (propped wall at top) and 15 (cantilever wall) with exaggerated scale for deformation by 10 times. Figure (5) shows the horizontal plastic strain contours in nonlinear runs in the study. The plastic strain contours can be used in evaluation of plastic zone behind the wall. Figures (6, 7, and 8) show horizontal stress distribution behind the wall and lateral wall movement for different conditions studied. The vertical stresses in the extreme fiber of

the wall soil-side are presented in Figure (9). Figure (10) shows the variation of the normalized bending moment (M/EI) with depth of wall, which reflects the same shape of bending moment diagram. Figure (11) shows the pressure distribution suggested by Goh (1993) (cited by Das [23]). The author proposed a pressure distribution diagram for cantilever diaphragm walls in sand shown in Figure (12). Example of cumulative iterations during final phase of convergence of run 15 is shown in Figure (13). Discussion of the results and different factors influence the behavior of the wall are presented in the following sections.

Influence of Wall Stiffness

The lateral deflection increased by about 100% by reducing wall stiffness 10 times (runs 5,14, and 15). The lateral deflection increased by about 10 % when the wall stiffness decreased by about 35% (compare run 5 and 6). These results reflect the nonlinear soil response to change in wall stiffness. It is important to note that the wall material nonlinearity is not taken into account.

Influence of Consideration of Geometric Nonlinearity in the Analysis

Influence of geometric nonlinearity is clear in case of low soil modulus and friction angle (compare run 1 and 2). Run 1 processed about 90% of load sub steps only, and then the solution did not converge (due to bad elements shape at top corner of deformed soil), when geometric nonlinearity turned off the solution converged in run 2. Same behavior observed between runs 14 and 15. With increase in soil modulus and friction angle as in runs 8 and 9 the influence of geometric nonlinearity is small on change in lateral deflection. Both solutions (runs 9 and 8) with and without consideration of geometric nonlinearity converged.

Influence of Wall Boundary Condition at Lower Tip of the Wall

When the lower end of the wall is restraints in x and y directions, the lateral deflection at top end reduced by about 2 % on comparison with free to move end. On the other hand, when the lower end of the wall free to move very small gap developed at lower end between soil and wall. However, this gap is within the tolerance of formulation of the contact element used in the analysis (compare runs 4 and 5).

Influence of Soil Friction Angle

Runs 4 and 9 shows the retaining system response when the friction angle increased from 35^o to 39^o the lateral deflection decreased by more than 50 % (note the change in soil modulus also) and the very small gap between soil and wall become at the top part of the wall. The lateral deflection increased by about 42% when the friction angle reduced from 35^o to 31^o (compare run 5 with geometric nonlinearity on and run1, note; the change in soil modulus also).

Influence of Variation of Soil Modulus with Depth

Runs 3 and 7 represent different variation of soil modulus with depth with constant value of friction angle for run 3 equal 31^o and for run 7 equal 35^o. The lateral deflection decreased by increase in the value of soil modulus (compare run 3 and 7, Table (1)). The increase of soil modulus with depth decreases the lateral deflection by about 20 % if compared with using the average value of soil modulus for all the soil profile (compare run 7 and 4, Table (1)).

Contact Friction Stiffness

The lateral deflection increased by about 2.5% when the contact friction stiffness decreased to 1/3 of its original value (compare runs 9 and 10, Table (1)). The difference in lateral deflection may be increased for lower value of soil modulus. The normal stiffness did not change between runs 9 and 10. In general both lateral deformations in runs 9 and 10 are small, which implies less lateral yielding of soil.

Influence of Restraint at Top of the Wall (Propped wall)

Restraining the top end of the wall reduces the lateral deformation by about 80%. The location of maximum horizontal displacement transferred close to the excavated level (compare runs 11 and 2, and runs 7 and 12) when retaining the top end.

Influence of Soil Nonlinearity

Comparison between response of the retaining system with elastic and nonlinear soil for propped wall (compare runs 11 and 13) shows that the difference in the lateral displacement of the two runs is very small. The soil did not yield because the restraint at top end of the wall, that gives a reason for that small difference in lateral displacement of the wall. The difference would have been larger if the wall was not propped at the top due to yielding of soil behind the wall.

Development of Plastic Strain in Soil Behind the Wall

In Rankin's theory (for smooth vertical wall) the entire semi-infinite mass being subjected to lateral expansion (active) or compression (passive). The movement of cantilever wall, however, cannot produce the passive or active state in the soil mass as a whole. The active state (see Figure (5) horizontal plastic strain for different runs) can be developed only within wedge of soil between the wall and failure plane, intersecting the lower end of the wall with an angle of $45+\phi/2$ to horizontal. The remnant of soil mass is in state of "elastic" equilibrium. A certain minimum value of lateral strain is necessary to develop the active plastic state within the mentioned wedge.

It is important to know that it is difficult in finite element to analyze a complete mass in failure state. Runs 9 and 10 do not deform laterally enough to produce the active state due to high friction angle and soil modulus see Table (1). Results of run 2, 4 and 15 produce more lateral displacement. From the results, it is found that the estimated value of soil elastic modulus is important factor influencing the results since the Drucker-Prager model do not change in size (isotropic hardening). The inclinations of contour lines with horizontal (Figure (5)), for all contours with horizontal plastic strain ≈ 0.01, are close to $45+\phi/2$. Coulomb assumed a plane failure surface, but due to wall friction the actual surface separates between elastic and plastic equilibrium regions is curved as mentioned in literature and shown by the results of horizontal plastic strain plotted in Figure (5). It is known that this assumption in coulomb's theory gives small error in active case.

Horizontal Stress Distribution Behind the Wall

The pressure distribution on a vertical plane behind the wall extracted from the results and plotted with depth for different runs as shown in Figures (6, 7, and 8). It can be shown that the pressure on the lower part of the wall lies between active pressure and at rest pressure. The pressure distribution on top part of the wall is close to active earth pressure and depends on wall stiffness, soil friction angle and soil modulus.

The following is quoted from the BS 8002 [6] standard:

The soil deformations, which accompany the full mobilization of shear strength in the surrounding soil, are large in comparison with the normally acceptable strains in service. Accordingly, for most earth retaining structures the serviceability limit state of displacement will be the governing criterion for a satisfactory equilibrium and not the ultimate limit state of overall stability. However, although it is generally impossible or impractical to calculate displacements directly, serviceability can be sufficiently assured by limiting the proportion of available strength actually mobilized in service". This shows the complexity of estimating the earth pressure distribution (as shown in Figures (6, 7, and 8)) that is due to nonlinear interaction of wall stiffness, soil friction angle, and soil modulus

Proposed Earth Pressure Distribution Behind a Cantilever Retaining wall

Das [23] cited the work by Goh (1993) for earth pressure distribution for conventional R.C retaining wall shown in Figure. (11). Based on the current study results, the author proposes an earth pressure distribution for cantilever diaphragm walls presented in Figure (12). For sand with $\varphi > 35^o$, the earth pressure on top part of the wall (to 0.75 H) follow Rankine earth pressure, and for deeper part of the wall the pressure increases linearly to become k_o pressure at lower end of the wall. For sand with $\varphi \leq 35^o$, the earth pressure follows Rankine distribution to depth from top = 1.25 H, then increase linearly to k_o value at lower end of the wall. The proposed earth pressure distribution by the author is in agreement with what was stated by BS 8002 [6] standard about the possible change in earth pressure distribution.

Wall Bending and Bending Stresses in the Wall

It is important to note that the deformation of an earth retaining structure has a direct effect upon the forces on the structure developed from the retained soil. The structural forces and bending moments due to earth pressures reduce as deformation of the structure increases.

Wall bending obtained from the vertical stresses on the extreme wall fiber faced with soil, is shown in Figure (9). Positive sign means tension in soil side of the wall and negative sign means tension on the excavation side of the wall (runs 11, and 12). The known relation $\sigma_y = M.y/I$ is used in computation of the normalized bending, which equal to moment gradient $d^2y/dx^2 = M/EI = \sigma_y/E.y$, for 0.5 m wall thickness with pure bending $M/EI = 4\sigma_y/E$. The normalized bending moment is used in Figure (10) to include the influence of wall stiffness EI on the value and shape of bending moment. The most flexible wall is used in run 15 shows a variation of bending moment from positive to negative. The large value of normalized bending moment at the lower end of the wall, due to constraint in wall movement in vertical direction, increases the vertical stress at lower end hence increasing the computed bending moments. If the lower hard boundary increased in depth under the wall end the resulted bending moment would be reduced. It would have been better to compute the bending moment by double differentiation of the deflection shape of the wall. Figure (10) reflects influence of all variables on the value and shape of bending moment. The shapes of normalized bending moment in lower part reflect the fixity of the wall. The fixity of the wall is varied for different runs according to φ, EI, and propped wall, which considered as the main variables, controlling the bending shape and value.

Solution Time and Convergence

Table (1) presents the time required for each run using computer Pentium III, 500 MHz. The cumulative number of iterations also presented. In general the number of iterations and time required for run increase by increase in lateral deflection of the wall. Figure (13) shows the iteration process at final part of convergence for run 15.

CONCLUSIONS

It should be emphasized on the coupled relation between the lateral deformation and the earth pressure distributions. Finite element models may be able to evaluate both deformation and stress. Several factors influence modeling and simulation of earth retaining structures are examined in this study using ANSYS finite element program. Gaps developed in some locations behind the wall were within tolerance. In other cases, it is found that when using geometric nonlinearity gaps were excluded. Influence of wall friction on earth pressure value as expressed in Coulomb analysis is not clearly observed with limited runs in these analyses. Contact element is a must in simulations of soil structure interactions. When geometric nonlinearity of the soil activated with contact nonlinearity few elements distorted in large deformation model and the solution stops. However, with less deformed models, the solutions converged. Lower tip restraint does not have much influence on wall behavior in this study since the wall penetration is large and the wall is considered as fixed in soil. The model shows the development of plastic strain in soil. Normalized bending curves for different runs as plotted in Figure (10) show influence of different factors. A proposal is suggested for earth pressure distribution for cantilever diaphragm wall is presented in Figure (12).

REFERENCES

[1] Terzaghi k., and Peck, R. B "Soil Mechanics in Engineering Practice" 2nd. Edn. Wiley New York. (1967)

[2] Peck, R. B. "Deep Excavations and Tunneling in Soft Ground," 7th *ICSMFE, State-of-Art Volume,* (1969), pp. 225 – 290.

[3] Mana A. I, and Clough, G. W. "Prediction of Movements for Braced Cuts in Clay", Journal ASCE, Vol. 107, No. GT6, (1981).

[4] ANSYS 5.4 "program Documentation" SAS IP, Inc. (1997).

[5] Craig, R. F. "Soil Mechanics" Van Nostramd Reinhold (UK) Co. Ltd, 3rd Edition, (1984)

[6] Code of Practic for Earth Retaing Structures 8002 (1994) British Standard, © BSI 12 September (2001).

[7] Potts, D. M., and Martins, J. P., "The Shaft Resistance of Axially Loaded Piles in Clay", Geotechnique, 32, No. 4, pp. 369-386, (1982).

[8] Ottaviani, M., and Marchetti, S., "Observed and Predicted Test Pile Behavior", Int. J. for Num. and Anal. Meths. in Geomech., 3, pp.131-143, (1979).

[9] Jardine, R. J., Potts, D. M., Fourie, A. B., and Burland, J. B., "Studies of the Influence of Non-linear Stress-Strain Characteristics in Soil-Structure Interaction", Geotechnique, 36, No. 3, pp. 337-396, (1986).

[10] Ananadarajah, A. M., and Dafalias, Y. F., "Bounding Surface Plasticity. III: Application to Anaisotropic Cohesive soils", J. of Engg. Mech. Div., ASCE, 112, No. 12, pp. 1292-1318, (1986).

[11] Banerjee, P. K., Stipho, A. S., and Yousif, N. B., "A Theoretical and Experimental Investigation of the Behavior of Anisotropically Consolidated

Clay", in Developments in Soil Mechanics and Foundation Engineering, Edited by P.K. Banerjee and R. Butterfield, Elsevier Applied Science Publishers, England, Vol. 2, Chap. 1, pp. 1-41, (1985).

[12] Mroz, Z., and Zienkiewicz, O. C., "Uniform Formulation of Constitutive Equations for Clays and Sands", in Mechanics of Engineering Materials, eds. C. S. Desai and R. H. Gallegher, John Wiley and Sons, pp. 415-449, (1984).

[13] Prevost, J. H., "Plasticity Theory for Soil Stress-Strain Behavior", J. of Engng. Mech. Div., ASCE, 104, No. EM5, pp. 1177-1194, (1978).

[14] Drucker, D. C, and Prager, W. "Soil Mechanics and Plastic Analysis or Limit Design" Quart. J. Appl. Math., vol. 10, (1952), pp. 157-165.

[15] Goodman, R. E., Taylor, R. L., and Brekke, T. L., "A model for the Mechanics of Jointed Rock", J. of Soil Mech. and Founds. Div., ASCE, Vol. 94, No. SM3, (1968), pp. 637-659.

[16] Zeinkiewicz, O. C., Best, B., Dullage, C., and Stagg, K. G., "Analysis on Non-linear Problems in Rock Mechanics with Particular reference to Jointed Rock Systems", Proc. 2nd. Int. Cong. On Rock mech., Belgrad, Vol. 3, (1970), pp. 501-509.

[17] Ghaboussi, J., Wilson, E. L., and Isenberg, J., "Finite Element for Rock Joints and Interfaces", J. of Soil Mech. and Founds. Div., ASCE, Vol. 99, No. SM10, (1973), pp. 833-848.

[18] Katona, M. G., "A simple Contact Friction Interface Element with Application to buried Culvert", Proc., Symp. On Implementation of computer Procedures and Stress-Strain Laws in Geotech. Eng., Chicago, Illinois, Vol. 1, (1981), pp. 45-63.

[19] Herrmann, L. R., "Finite Element Analysis of Contact Problems", J. of Eng. Mech. Div., ASCE, Vol. 104, No. EM5, (1978), pp. 1043-1057.

[20] Desai, C. S., Zaman, M. M., Lightner, J. G., and Siriwardane, H. J., "Thin Layer Elements for Interfaces and Joints", Int. J. for Num. and Anal. Meths. in Geomech., Vol. 8, No. 1, (1984), pp. 19-43.

[21] Wilson, E. L., "Finite Elements for Foundations, Joints and Fluids", Finite Elements in Geomech., Edited by G. Gudehus, John Wiley and Sons, New York, (1977), pp. 319-350.

[22] Pande, G. N., and Sharma, K. G., "On Joint/Interface Elements and Associated Problems on Numerical Ill-conditioning", Int. J. for Num. and Anal. Meths. in Geomech., Vol. 3, No. 3, (1979), pp. 293-300.

[23] Das, B.M. "Principal of Foundation Engineering" New York. PWS-KENT Publishing Company, Boston, 2nd Edition. (1996).

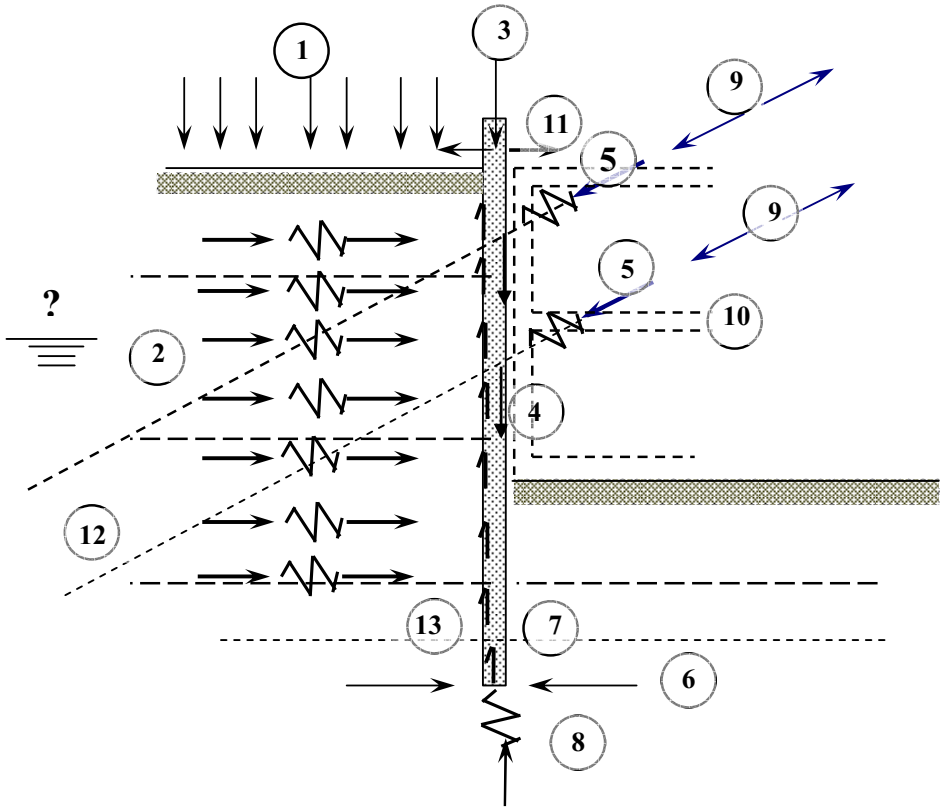

1- External Surface Load (if exist)
2- Soil Lateral Pressure (Water table and hydrostatic Pressure)
3- Vertical Load on Top of the Wall (may be prestressed Vertical wall)
4- Vertical Load from Basement Slabs (if exist)
5- Tie-back Prestressing (Staged Excavation and Construction Procedure) (if exist)
6- End Lateral Restrained Conditions
7- Wall Rigidity
8- Vertical Stiffness at Tip of the Wall
9- Long Term Behavior of Tie-back Anchors
10- Interaction with Basement Wall (Permanent or Temporary System)- (if exist)
11- Wall Lateral Movement allowed or happened (in relation to soil strength)
12- Soil Layers Difference in Properties
13- Wall-Soil Friction

Figure 1: Soil – Wall – Load – Structure Nonlinear Interaction

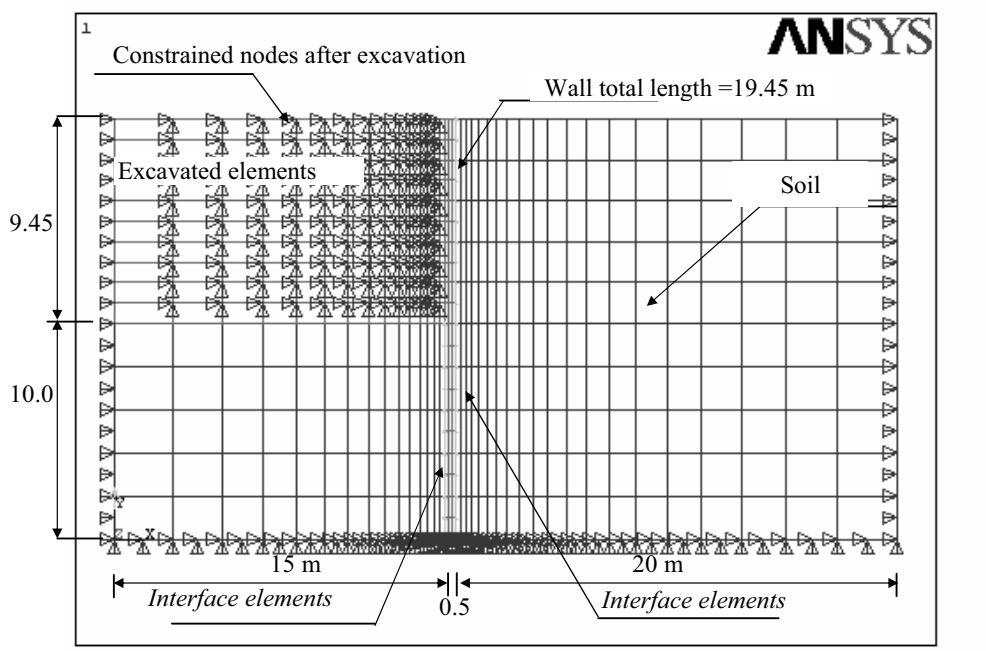

Figure 2: Finite Element Mesh Used in the Study

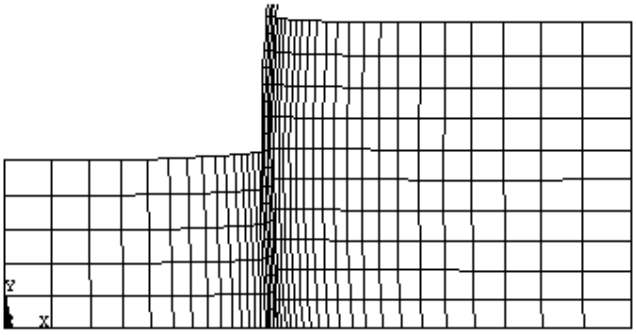

Figure 3: Deformed Shape Run-11 (Propped at Top), Displacement x 10

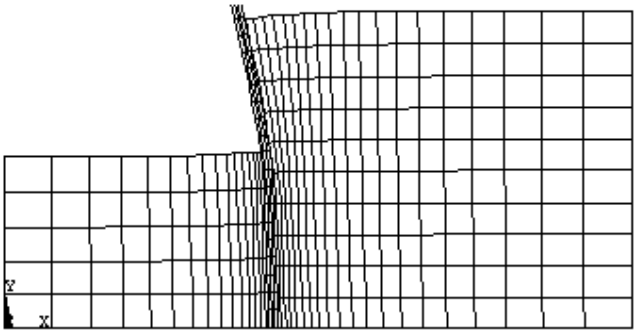

Figure 4: Deformed Shape Run-15, Displacement x10

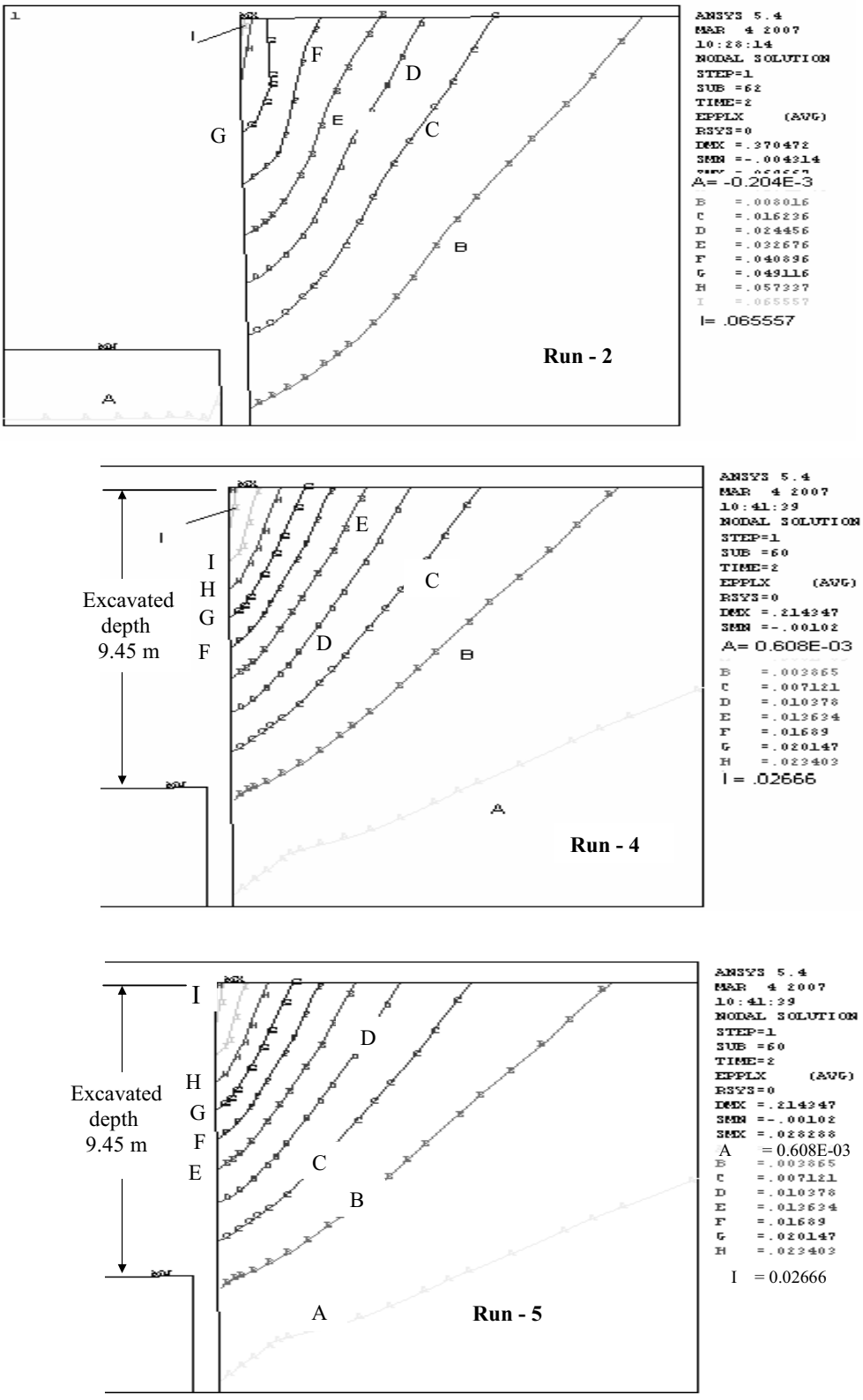

Figure 5: Contour lines of Horizontal Plastic Strain in Soil Plotted on Deformed Shape

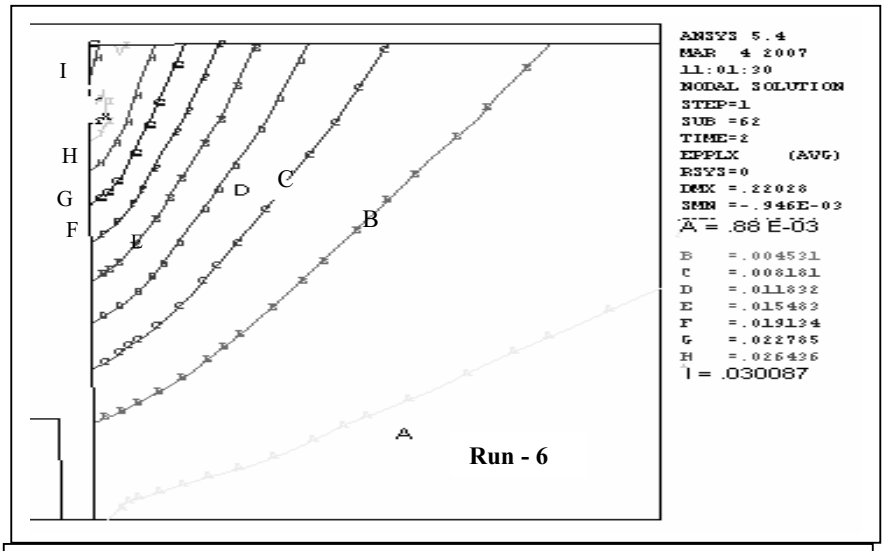

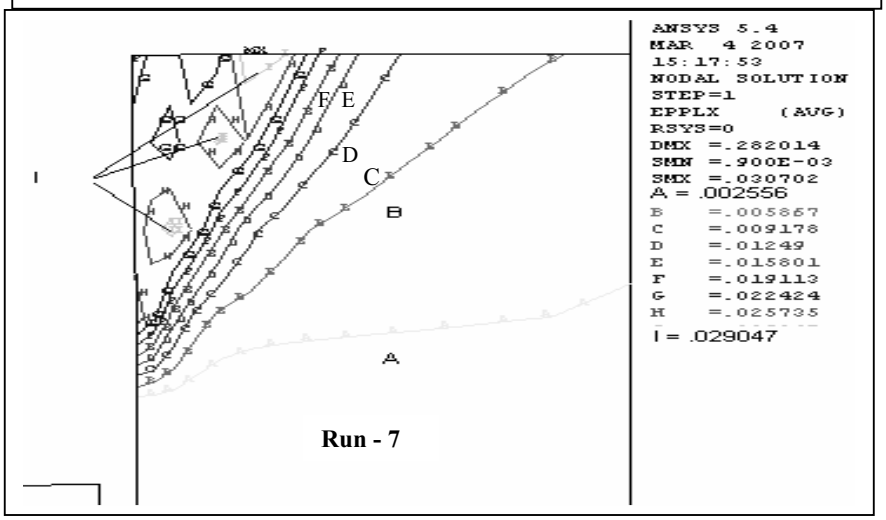

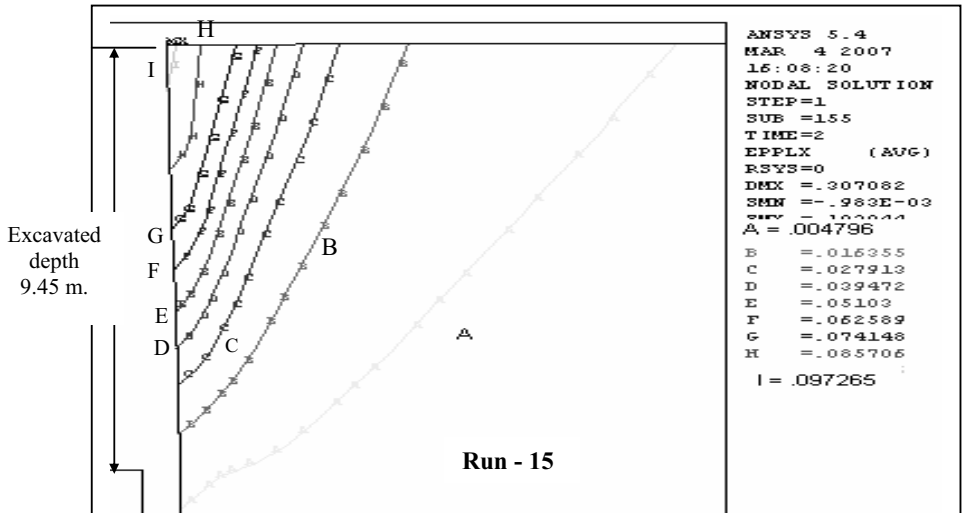

Figure 5: (continue) Contour lines of Horizontal Plastic Strain in Soil Plotted on Deformed Shape

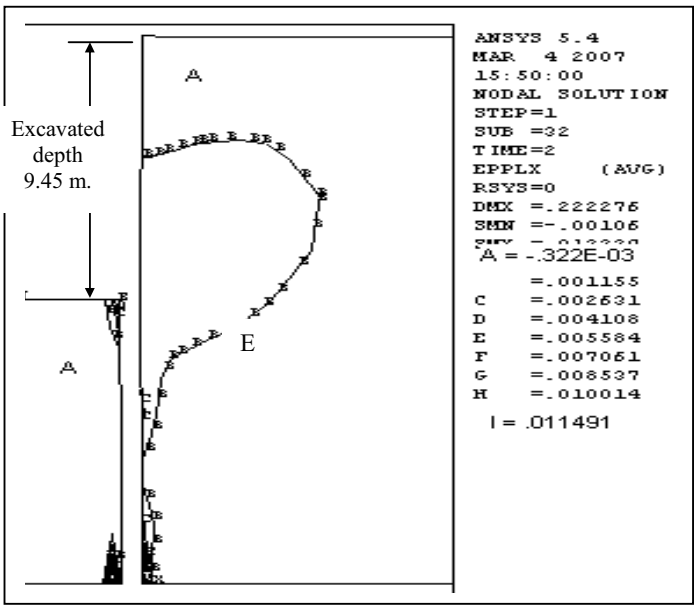

Figure 5: (continue) Contour lines Horizontal Plastic Strain in Soil Plotted on Deformed Shape

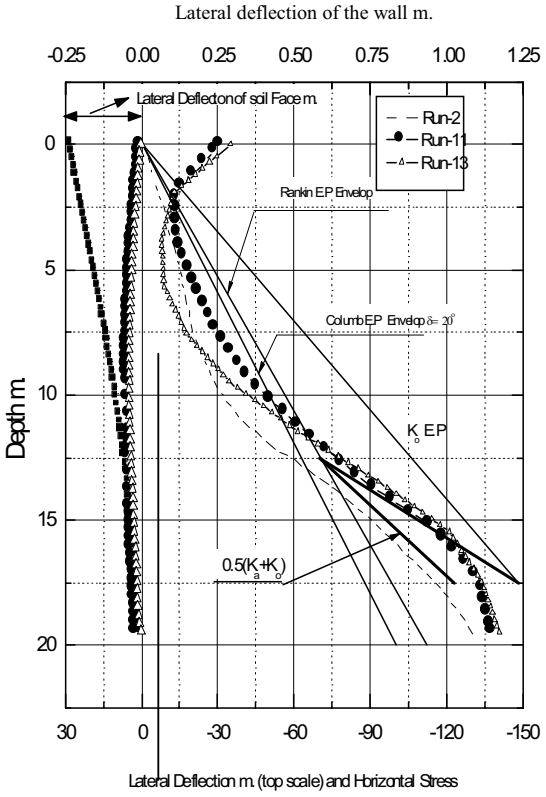

Figure 6: Lateral Deflection and Horizontal Stresses, $\varphi = 31^o$

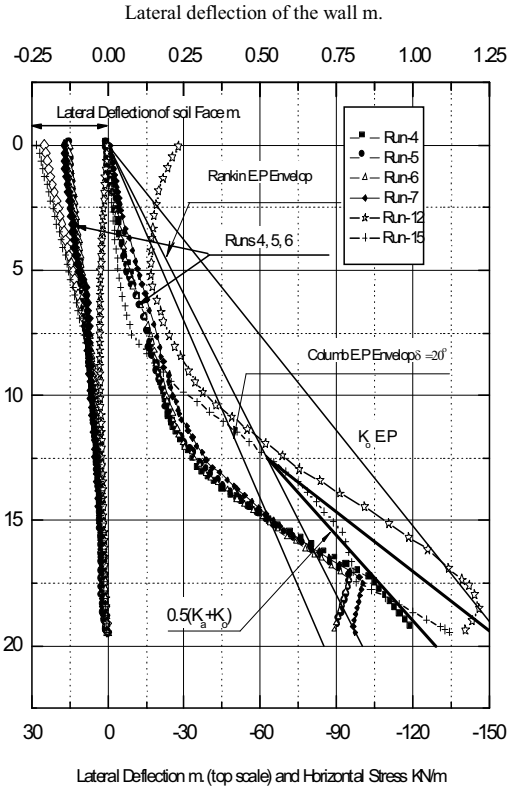

Figure 7: Lateral Deflection and Horizontal Stresses, $\varphi = 35^o$

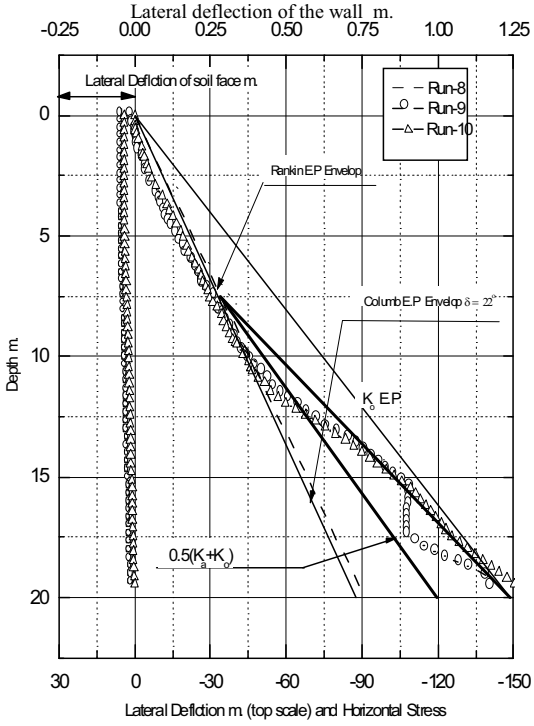

Figure 8: Lateral Deflection and Horizontal Stress φ = 39°

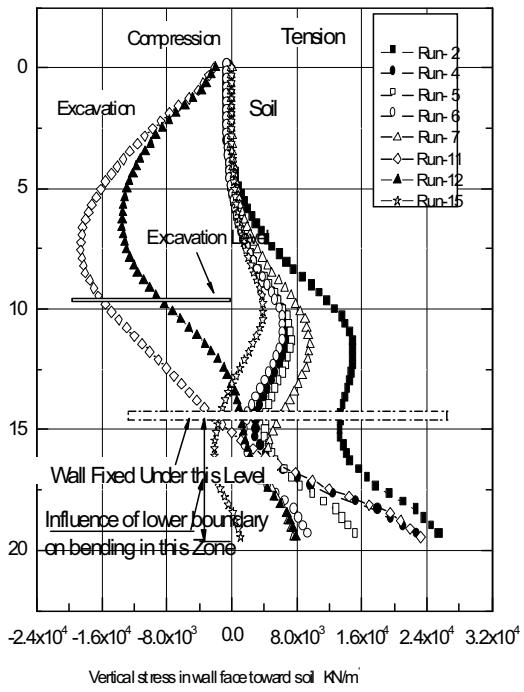

Figure 9: Vertical Stresses in Extreme Fiber of the wall

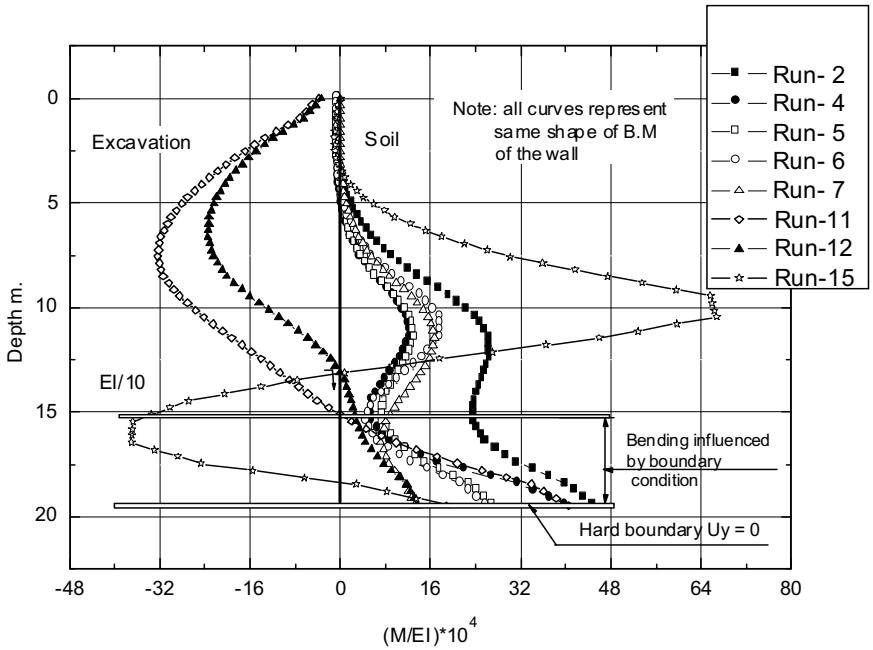

Figure 10: Variation of Normalized Bending Moment with Depth

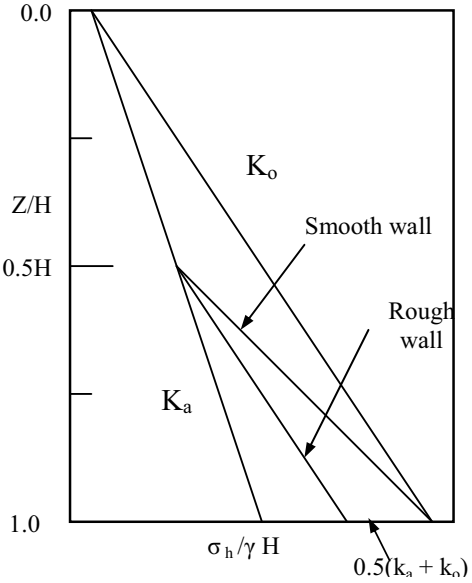

Figure 11: Proposed earth pressure distribution by Goh (1993)

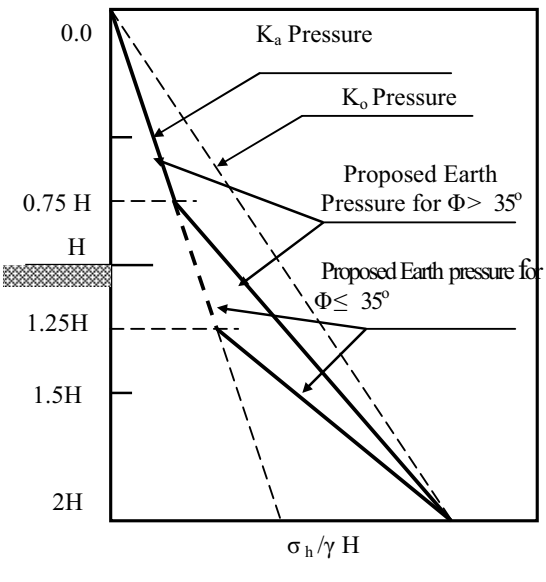

Figure 12: Proposed earth Pressure Distribution by the Author for Cantilever Diaphragm Wall

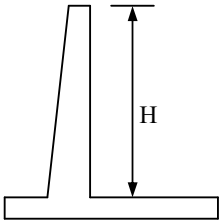

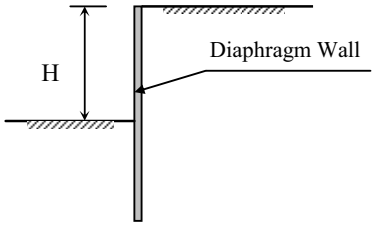

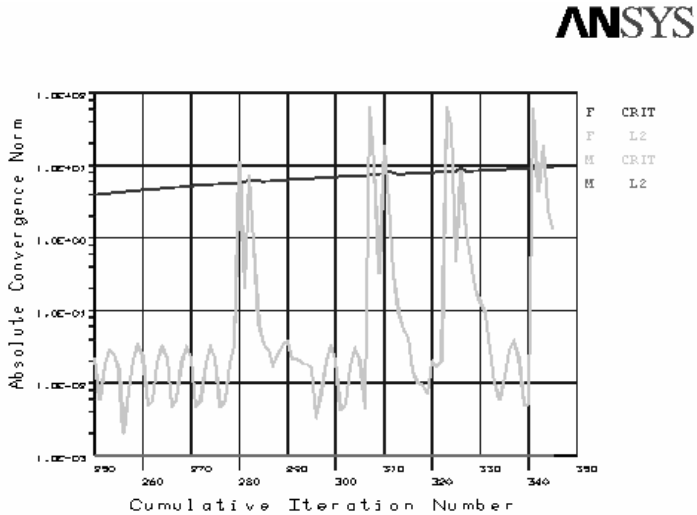

Figure 13: Final Part of cumulative iterations for converged solution of Run 15